



Published in final edited form as:

*J Biomed Mater Res A*. 2009 February ; 88(2): 503–519. doi:10.1002/jbm.a.31886.

## Adsorbed serum albumin is permissive to macrophage attachment to perfluorocarbon polymer surfaces in culture

M.L. Godek<sup>1</sup>, R. Michel<sup>2</sup>, L. M. Chamberlain<sup>1</sup>, D. G. Castner<sup>2</sup>, and D.W. Grainger<sup>1,3,\*</sup>

<sup>1</sup>Cell and Molecular Biology Program, Colorado State University, Fort Collins, CO 80523-1872 USA

<sup>2</sup>National ESCA and Surface Analysis Center for Biomedical Problems, Departments of Bioengineering and Chemical Engineering, University of Washington, Seattle, WA 98195-1750 USA

<sup>3</sup>Departments of Pharmaceutics and Pharmaceutical Chemistry, and Bioengineering, University of Utah, Salt Lake City, UT 84112-5820 USA

### Abstract

Monocyte/macrophage adhesion to biomaterials, correlated with foreign body response, occurs through protein-mediated surface interactions. Albumin-selective perfluorocarbon (FC) biomaterials are generally poorly cell-conducive due to insufficient receptor-mediated surface interactions, but macrophages bind to albumin-coated substrates and also *preferentially* to highly hydrophobic fluorinated surfaces.

Bone marrow macrophages (BMMO) and IC-21, RAW 264.7 and J774A.1 monocyte/macrophage cells were cultured on FC surfaces. Protein deposition onto two distinct FC surfaces from complex and single-component solutions was tracked using fluorescence and time-of-flight secondary ion mass spectrometry (ToF-SIMS) methods. Cell adhesion and growth on protein pre-treated substrates were compared by light microscopy. Flow cytometry and integrin-directed antibody receptor blocking assessed integrins critical for monocyte/macrophage adhesion *in vitro*.

Albumin predominantly adsorbs onto both FC surfaces from 10% serum. In cultures pre-adsorbed with albumin or serum-dilutions, BMMO responded similar to IC-21 at early time points. Compared to Teflon<sup>®</sup> AF, plasma-polymerized FC was less permissive to extended cell proliferation. The  $\alpha_2$  integrins play major roles in macrophage adhesion to FC surfaces: antibody blocking significantly disrupted cell adhesion. Albumin-mediated cell adhesion mechanisms to FC surfaces could not be clarified. Primary BMMO and secondary IC-21 macrophages behave similarly on FC surfaces, regardless of pre-adsorbed protein biasing, with respect to adhesion, cell morphology, motility and proliferation.

### Keywords

perfluorocarbon; foreign body reaction; integrin blocking; cell line; serum proteins

### INTRODUCTION

Macrophages are key mediators of host inflammatory responses to surgically placed biomedical devices, implicated in an abnormal wound healing response commonly observed around implanted materials known as “foreign body reactions” (FBR).<sup>1–3</sup> Macrophage cells

\* to whom correspondence should be addressed: david.grainger@utah.edu.

represent a highly adaptable, dynamic cell population with the ability to respond to activating cues of both chemical and physical nature present in their local environment. Foreign body giant cells, the fusion product of monocytes and macrophages and one cellular hallmark of the FBR to implantable materials,<sup>4</sup> are frequently found at surfaces of biomaterial implants, and material surface chemistries have been shown to influence fusion.<sup>5</sup> Modulating events that facilitate progression of the FBR at implant sites remains of substantial interest toward improved biomedical device performance and host integration. To date, little *in vivo* control over this complex reaction to implanted materials has been demonstrated.

This study focused on well-known influences on cell adhesion by surface chemistry and the adsorbed protein layer.<sup>5–7</sup> *In vivo*, biomaterials surfaces are instantly and continuously bombarded with thousands of different host proteins,<sup>8–12</sup> and surface chemistry is recognized to exert an influence on adsorbed protein composition, exchange dynamics and structural conformations.<sup>13–15</sup> *In vitro*, surface-denatured proteins lead to increased monocyte adhesion,<sup>16</sup> the first step in a sequence of events that may ultimately result in a FBR *in vivo*. As the predominant plasma protein,<sup>8,9</sup> albumin's surface interaction has been studied extensively<sup>17–26</sup> due to albumin's propensity to reduce many biological interactions with surfaces, including reduced thrombogenicity of polymers,<sup>18</sup> decreased bacterial adhesion and device-centered infections,<sup>18</sup> reduced platelet adhesion<sup>27–29</sup> and limited cell adhesion.<sup>30</sup>

Albumin has been shown to bind strongly and selectively, to perfluorinated (i.e., plasma deposited and poly(tetrafluoroethylene) or PTFE) surfaces,<sup>24</sup> out-competing cell-adhesive extracellular matrix (ECM) proteins like fibronectin in adsorption from binary solutions and serum dilutions, even when fibronectin bulk concentration is biased 10–100 times higher than found physiologically.<sup>31</sup> Albumin apparently “masks” adsorbed fibronectin, and low rates of endothelial cell adhesion have been correlated to a limiting adsorbed fibronectin surface density as probed by radiolabeling and anti-fibronectin antibodies.<sup>31</sup> In fact, poor cell adhesion to perfluorinated surfaces has been reported for multiple different cell types.<sup>32–36</sup> Thus, increased density of surface-adsorbed albumin on these surfaces correlates to reduced mammalian cell adhesion<sup>30</sup> for numerous cell types with important consequences *in vivo*. Surfaces that “select” albumin from complex biological milieu, such as perfluorocarbons,<sup>24,31</sup> are predicted to be poorly supportive of cellular adhesion given that most cells are not known to have specific receptors to actively engage albumin in adhesion. Notably, hepatocytes,<sup>37</sup> vascular endothelial cells,<sup>38</sup> and monocytes, macrophage and dendritic cells<sup>39,40</sup> have been reported to be exceptions. For example, the FcRN receptor, identified as an albumin-binding protein present on monocyte, macrophage and dendritic cells,<sup>40</sup> binds exclusively at pHs below 6.5 but is not a known cell-adhesive receptor physiologically.<sup>39</sup> Hence, in the context of the FBR, highly albumin-adsorbed perfluorinated surfaces might be predicted to elicit reduced inflammatory cell activation if cell-surface adhesion is inhibited. Surprisingly, *in vitro* cultures of murine primary- and secondary-derived monocyte-macrophage cells have been shown to adhere, grow and proliferate proficiently on hydrophobic (i.e., polystyrene) and perfluorocarbon (e.g., Teflon® AF, plasma-polymerized FC, fluorinated ethylene propylene) substrates.<sup>41–44</sup>

This study sought to 1) examine and compare aspects of cell adhesion behavior for murine cells of primary- (BMMO) and secondary- (IC-21, J774A.1, RAW 264.7) origins when grown on perfluorinated (i.e., fluorocarbon, FC) surfaces *in vitro*, and 2) to propose a mechanism by which initial monocyte/macrophage cell adhesion events occur on FC surfaces in the context of establishing a FBR to biomaterials. For practical purposes and to allow an appropriate equivalence comparison between primary and secondary derived macrophages, this study focused on responses of BMMO and IC-21 cells exclusively. Of the

three secondary cell lines initially tested, IC-21 was selected as a best match for comparison to primary BMMO because: 1) IC-21 represents the most physiologically relevant cell line within this group,<sup>45</sup> and 2) mature IC-21 cell size, morphology, adhesion and spreading behaviors were shown to be very similar to BMMO. To contrast (monocyte-) macrophage cell behavior on FC surfaces, NIH 3T3 fibroblasts, an attachment-dependent cell type but non-adhesive to fluorocarbon surfaces *in vitro*,<sup>36,44</sup> was used as a control. The  $\alpha_2$  integrin family, vital to development of the inflammatory response *in vivo*<sup>46</sup> and known to interact with specific ECM proteins as well as denatured proteins at surfaces,<sup>16</sup> was hypothesized to be the primary mediator of any observed initial macrophage adhesion to FC surfaces exposed to biological milieu *in vitro*. Further, as macrophages are known to secrete fibronectin,<sup>47-50</sup> this was also studied as it may facilitate monocyte and macrophage adhesion to FC surfaces via endogenous ECM production, deposition and cell-based remodeling of the pre-existing adsorbed protein layer.

## MATERIALS AND METHODS

### Culture surface preparation for Time-of-Flight Secondary Ion Mass Spectrometry Analysis

Polystyrene (PS) dishes were cut into pieces (~ 1 cm × 1 cm), labeled to indicate “bottom” and affixed to the bottom of PS petri dishes using double-sided tape, or left unfixed to free-float in protein milieu. All Teflon<sup>®</sup> AF culture surfaces were prepared by evaporation deposition; fluorocarbon content was subsequently confirmed via x-ray photoelectron spectroscopy (XPS) analysis as described previously.<sup>32</sup> Briefly, sufficient Teflon<sup>®</sup> AF (DuPont Fluoroproducts) solution (0.1 wt.% in FC-40 solvent, 3M Corp.) was added to these petri dishes to completely cover all fixed PS pieces. Coated PS surfaces were placed in a vacuum oven overnight at 65°C to remove residual solvent, and plates were misted with 70% ethanol, dried, and treated with biosafety cabinet UV light for 20 minutes immediately before culture, a process shown to sterilize while remaining benign to cell culture surface chemistry.<sup>44</sup> Teflon<sup>®</sup> AF samples were also reserved as controls. Following sterilization, samples were immersed in either a 3 mg/ml bovine serum albumin (BSA) solution (fraction V, OmniPur<sup>®</sup>, Sigma, 98% pure by gel electrophoresis) or 10% fetal bovine serum (FBS) solution, both in sterile Dulbecco’s phosphate buffered saline with  $\text{Ca}^{2+}$  and  $\text{Mg}^{2+}$  (PBS<sup>++</sup>), and incubated at 37°C for 24 hours. Samples were removed, rinsed twice with PBS<sup>++</sup>, three times with 18 M “Nanopure-grade” ASTM I water and dried under a stream of nitrogen. These samples were subjected to surface analysis as described below.

### Preparation of fluoropolymer culture surfaces using plasma deposition

All plasma-prepared fluorocarbon (pp-FC) surfaces employed in these studies were gifts of Dr. E. Fisher and Dr. G. Malkov (Colorado State University, USA), prepared and characterized as previously described.<sup>44</sup> This method produces a robust (100 nm) thick film of crosslinked perfluorocarbon highly enriched in both -CF<sub>2</sub> and -CF<sub>3</sub> groups. Briefly, all films were deposited in a home-built inductively coupled radio frequency (RF) (13.56 MHz) plasma reactor.<sup>51</sup> Pulse duty cycle was varied using the internal pulse generator of an RF power supply. Peak applied RF pulse power ( $P$ ) was kept constant at 300W for FC films. For all experiments, C<sub>3</sub>F<sub>8</sub> (Air Products, 99%) gas flow was kept constant at 10.0 sccm (standard cubic centimeters per minute), resulting in a reactor pressure of ~200 mTorr.

### Time-of-Flight Secondary Ion Mass Spectrometry (ToF-SIMS) analysis

A Physical Electronics 7200 instrument with an 8 keV Cs<sup>+</sup> ion source, a reflectron time-of-flight mass analyzer, chevron-type multi-channel plates, and a time-to-digital converter was used for data acquisition. Data was acquired for the Teflon<sup>®</sup> AF samples after incubation (as described above) with 3 mg/ml BSA or 10% FBS; other protein spectra for comparison were collected previously.<sup>21,52,53</sup> Positive secondary ions mass spectra were acquired over a mass

range from  $m/z = 0$  to 1000. Negative ion ToF-SIMS spectra were not considered here due to a lack of unique peaks for the different amino acids.<sup>54</sup> Each spectrum analyzed an area of  $100 \mu\text{m} \times 100 \mu\text{m}$ , and the total ion dose used to acquire each spectrum was less than  $1 \times 10^{12}$  ions/cm<sup>2</sup>. Mass resolution ( $m/m$ ) of the secondary ion peaks in the positive spectra was typically between 3000 and 5000. The ion beam was moved to a different spot on the sample for each acquisition. Positive spectra were calibrated to the  $\text{CH}_3^+$ ,  $\text{C}_2\text{H}_3^+$ ,  $\text{C}_3\text{H}_5^+$ , and  $\text{C}_5\text{H}_{10}\text{N}^+$  peaks before any further analysis. At least two replicates were prepared for each sample type, with three spectra acquired from each replicate.

### Principal Components Analysis (PCA) of ToF-SIMS data

PCA was used to analyze the positive ToF-SIMS data from protein-adsorbed surfaces using scripts written at NESAC/BIO (University of Washington, USA) for MATLAB (The MathWorks, Inc.). All spectral processing (peak selection, normalization, PCA, etc.) was done as described previously.<sup>21</sup> Briefly, each amino acid was assigned a distinct mass peak, and the abundance of each peak, or amino acid, respectively, was used as input for the dataset. PCA yields an output of both a “scores” and a “loadings” plot.<sup>55</sup> The scores plot shows the relationship among samples and the loadings plot shows the relationship between the new principal components (PCs) and the original ToF-SIMS peaks. Wagner *et al.*<sup>21</sup> demonstrated that proteins present at a surface can be identified through unique amino acid fragmentation patterns in the ToF-SIMS positive ion spectra. Here, the ToF-SIMS data from BSA and 10% FBS adsorbed onto Teflon<sup>®</sup> AF surfaces was projected into the data set of Wagner *et al.*<sup>21</sup>. In addition to PCA, other multivariate analysis methods such as discriminant analysis and neural networks have been used to classify different adsorbed protein films.<sup>53,56</sup>

### Fluorescence labeling of proteins for detection of surface adsorption

Fibronectin (from bovine plasma, Sigma) and BSA solutions were fluorescently labeled and subsequently purified per manufacturer’s instructions using Alexa Fluor 555<sup>®</sup> and Alexa Fluor 647<sup>®</sup> protein labeling kits (Invitrogen). Protein and dye concentrations were determined by optical density using UV-vis spectroscopy. Subsequently, samples of pp-FC, Teflon<sup>®</sup> AF, negative control Codelink<sup>™</sup> activated hydrogel-coated slides (Amersham Biosciences) or glass coverslips (positive control) were either completely covered with dye-labeled protein solution (depending on the substrate size: small samples were completely immersed, while wax pencil “wells” were drawn on larger slides), or spotted with 30  $\mu\text{l}$  drops (confined within a wax pencil-defined well). Samples were exposed to: 1) single component solutions of fluorescently labeled albumin or fibronectin, or 2) a mixture of both dye-labeled proteins (each with a different fluorescent label) in a range of sample concentrations (albumin, from 1.5  $\mu\text{g}/\text{ml}$  to 1.5  $\text{mg}/\text{ml}$ ; fibronectin, from 1.9  $\mu\text{g}/\text{ml}$  to 1.9  $\text{mg}/\text{ml}$ ) or 3) a mixture of both proteins with only one dye-labeled protein in the same range of sample concentrations (*vide supra*). Coverslips were transferred to petri dishes and incubated at 37°C, 98% humidity for 24 hours. No differences in 30  $\mu\text{l}$  spot sizes were discernable after the 24 hour incubation period (i.e., negligible evaporation) when the remaining solution was rinsed from the surface using PBS<sup>++</sup>, further rinsed copiously with PBS<sup>++</sup>, dried under nitrogen and affixed to glass slides using double-sided tape (edges only). Samples were scanned for fluorescence signal using a Perkin Elmer ScanArray Express<sup>™</sup> Microarray Scanner employing appropriate optical filters and wavelengths for each dye employed. Gain and power settings were consistently controlled for sample comparisons. Images were processed for relative fluorescence intensity using ImagePro<sup>™</sup> software, and quantified using Quantity One<sup>®</sup> (Bio-Rad) and MS<sup>™</sup> Excel software.

## Cell culture

All cell lines were obtained from the American Type Culture Collection (ATCC, Manassas, VA). Cells were cultured in Dulbecco's modified Eagle's medium (DMEM, Mediatech, for J774A.1 and NIH 3T3) or RPMI 1640 (Mediatech, for IC-21 and RAW 264.7) supplemented with 10% FBS (HyClone, Inc.), and 1% penicillin-streptomycin (Life Technologies). Cultures were maintained in T-175 tissue culture polystyrene (TCPS) flasks (Nunc™) under standard conditions: incubation at 37° C, 98% humidity and 5% CO<sub>2</sub>. Cells were dissociated from culture flasks by incubation with Ca<sup>2+</sup>- and Mg<sup>2+</sup>- free cell culture grade HBSS (Life Technologies) (NIH 3T3), or by scraping with a rubber policeman (IC-21). Cell concentration and viability was assessed using standard trypan blue (BioWhittaker) dye exclusion assay and a hemacytometer.<sup>57</sup> All cell line subcultures were 25 beyond the passage number as received from ATCC.

## Primary cell harvest

BMMO were prepared from bone marrow cells harvested from the femurs and tibias of C57BL/6 mice.<sup>58</sup> To differentiate bone marrow stromal precursors into macrophages, bone marrow-extracted cells were cultured in "complete" bone marrow medium: DMEM supplemented with 10% L929 fibroblast-conditioned medium, 2 mM L-glutamine, 0.01% HEPES, 1% penicillin-streptomycin, and 2 mM non-essential amino acids (Sigma-Aldrich). Cells were grown under standard conditions (*vida supra*) with media changes every two days. This method has been shown to reliably produce differentiated macrophages.<sup>58</sup>

## Cell culture on model surfaces

TCPS (Falcon®, Becton Dickinson) and suspension culture PS (Corning Inc.) 15 × 100 mm dishes and 24-well plates were utilized for both control and experimental conditions. Teflon® AF fluoropolymer culture surfaces were prepared by coating PS surfaces as described (*vida supra*). Plates were tested for the presence of contaminating endotoxin using a Pyrogene™ Assay kit (Cambrex), and endotoxin levels were determined to be below the kit detection limit (0.02 EU/ml). Plates were subsequently preconditioned with appropriate medium containing 10% FBS for a minimum of six hours before cell seeding unless otherwise indicated. Cells were seeded at concentrations ranging from 5.0 × 10<sup>4</sup> to 3 × 10<sup>6</sup> cells per plate in fresh medium unless otherwise indicated. Initial seeding densities varied slightly for each cell type, due to surface-dependent differences in cell adhesion and growth rates, and to create roughly equivalent cell culture density time endpoints whenever possible.

## Protein pre-conditioning and cell culture on select surfaces

FC surfaces were incubated at 37°C for 24 hours with one of the following solutions: PBS<sup>++</sup>, 3 mg/ml BSA in PBS<sup>++</sup>, 0.3 mg/ml fibrinogen (bovine fraction 1, 75% clottable, ICN Biomedical), 10% FBS in PBS<sup>++</sup>, 10% heat inactivated (HI, 56°C, 1 hour) FBS in PBS<sup>++</sup>, 100% FBS or (cell specific) medium containing 10% FBS. At 24 hours, the protein solution or serum was removed by aspiration and cells were immediately seeded in an appropriate cell culture medium containing 10% FBS. Cell culture conditions proceeded as described above.

## Phase contrast microscopy

Images of cells on surfaces were obtained with either a Nikon Eclipse TS100 or a Nikon TMS inverted microscope using Nikon objectives. A Kodak DC290 camera was used to capture field images that were subsequently processed using Adobe Photoshop 6.0 (Adobe Systems, Inc.).



## Flow cytometry

Cells were pelleted by centrifugation (300 ×g, 5 minutes) and resuspended in 100 µl of staining solution (1% FBS, 0.01% NaN<sub>3</sub> in PBS<sup>++</sup>) with 1 µg of anti-CD16/32 (clone 93) mAb (eBioscience, F<sub>c</sub> receptor block). Cell F<sub>c</sub> receptors were blocked for 15 minutes at 4°C. Subsequently, cells were rinsed twice and resuspended in staining solution without antibodies. Cells were transferred to a 96-well plate for subsequent staining with 0.1 µg/ml of one of the following fluorescently conjugated (allophycocyanin, APC or fluorescein isothiocyanate, FITC) mAb per experiment: anti-CD11b (clone M1/70, APC), anti-IgG2a (clone eBR2a, FITC), anti-CD18 (clone M18/2, FITC), all eBioscience). Cells were stained for 30 minutes at 4°C, rinsed twice and resuspended in 500 µl staining solution without antibodies. Cell suspensions were analyzed on a FACSCalibur™ flow cytometer (BD) and data analysis was performed using Dako Cytomation Summit v 4.0 software.

## Integrin blocking studies

Function-blocking monoclonal antibodies (mAb, all sterile-filtered, azide-free, low endotoxin) directed against the murine integrin  $\alpha 2$  (M18/2) chain and a non-specific isotype-matched control (Rat IgG2a, ) were purchased from eBioscience. BMMO (matured 7 days) and IC-21 cells were pre-incubated for 30 minutes at 4°C with either an integrin-directed mAb or an appropriate isotype control (both 100 µg/ml). Cells were seeded into Teflon® AF-coated wells (2 cm<sup>2</sup>) previously treated for 24 hours with 10% FBS in PBS<sup>++</sup> at a density of 500 cells/mm<sup>2</sup> and allowed to adhere for 1 hour. After the 1 hour incubation period, non-adherent cells were removed with two 0.65 ml washes of warm (37°C) PBS<sup>++</sup>. Cells were fixed and stained according to the Wright-Giemsa method<sup>59</sup> using a commercially available kit (Hema 3® Staining System, Fisher). For each sample, adhesion blocking was evaluated by counting the number of cells in three lower-power fields and expressing the result as a percentage of untreated cells (Teflon® AF control). For each cell type, 4 independent experiments were performed, and data presented is the average of the 4 trials. Error was reported as standard error of the mean.

## Reverse transcriptase-polymerase chain reaction (RT-PCR)

Total RNA from BMMO and IC-21 cells grown on either TCPS or Teflon® AF surfaces was extracted and purified at various time points using RNeasy™ kits (Qiagen) per the manufacturer's instructions. First strand cDNA was synthesized from up to 4 µg of total RNA using Superscript II™ reverse transcriptase (Invitrogen) as recommended by the supplier. Both poly dT (Invitrogen) and murine fibronectin-specific primers<sup>60</sup> (5' - AGCAGTGGGAACGGACCTAC-3', 5' -GTAGGACGTCCCAGCAGC-3', IDT), 100 pmol per reaction, were used to obtain total and fibronectin-specific product cDNA, respectively. Primer-specific PCR amplifications of glyceraldehyde-3-phosphate dehydrogenase (GAPDH) served as "housekeeping" controls for each sample (5' - AACTTTGGCATTGTGGAAGGGCTC-3', 5' -TGGAAGAGTGGGAGTTGCTGTTGA-3'). Primers were either designed using Primerquest™ software (GAPDH) or as described previously (fibronectin).<sup>60</sup> All PCR amplifications were performed using an iTaq™ DNA polymerase kit (Bio-Rad) per manufacturer's instructions, on an iCycler thermal cycler (Bio-Rad). Each experiment was performed with 2 separate RNA isolations. PCR products were analyzed on 2% agarose gels, stained with ethidium bromide, and visualized/analyzed using a ChemiDoc XRS system (Bio-Rad) and Quantity One® software (Bio-Rad).

## RESULTS

### ToF-SIMS and PCA indicate albumin is the major protein component adsorbed to Teflon<sup>®</sup> AF substrates from 10% serum or pure albumin solutions

ToF-SIMS and PCA methods previously described have been frequently employed to classify and distinguish surface adsorbed proteins.<sup>21,52–54</sup> ToF-SIMS data are challenging to interpret due to the highly energetic SIMS ion fragmentation process that produces extensive fragmentation from surface species generating hundreds of peaks in the spectra from a sampling depth of approximately 1–2nm.<sup>61</sup> To facilitate protein identification under these experimental conditions, each amino acid can be assigned one or more characteristic mass peaks; a standard table of mass peaks assigned to specific amino acids has been established.<sup>21,54</sup>

PCA methods can be used to identify trends in large, complex data sets<sup>61</sup> and have been useful for identifying proteins adsorbed to surfaces,<sup>21,54</sup> including BSA, fibrinogen, fibronectin, IgG and others (Figure 1A). PCA's mathematical transformations relate a large number of (potentially) correlated variables into a smaller number of uncorrelated variables, i.e. the principal components (PCs). The first PC (x axis) is the PC that accounts for of the largest amount of variability in the data set (for cases reported here, 51%). The second PC (y axis) accounts for the next largest amount of variability in the dataset (here, 17%). In Wagner's model,<sup>21</sup> as presented here, this allows for qualitative statements to be made about the presence (or absence) of specific protein species on the tested surfaces, the intent of our use of this method here.

The PCA model of Wagner *et al*<sup>21</sup> was utilized for analysis of new ToF-SIMS protein data of interest (e.g., albumin) on Teflon<sup>®</sup> AF surfaces pre-treated with either complex (10% FBS) or single component (BSA) protein solutions. Data obtained for BSA were compared to results obtained by Wagner *et al*<sup>21</sup> (Figure 1A) for numerous single proteins adsorbed onto a PTFE surface. In this model the ellipses represent the 95% confidence interval for each protein, and most of the proteins (differing in amino acid composition) can be distinguished based on the two principal components shown (Figure 1A). Comparison supports the assertion that BSA present on Teflon<sup>®</sup> AF surfaces exposed to a single-component BSA solution (indicated as BSA<sub>Teflon AF</sub>) is highly similar to BSA results for PTFE and BSA on other surfaces (Figure 1B). In fact, data for all BSA samples shown (0.1 mg/ml BSA solution on mica,<sup>21</sup> silica (SiO<sub>2</sub>),<sup>53</sup> and plasma-polymerized poly(*N*-isopropyl acrylamide), (ppNIPAM),<sup>49</sup> are within the 95% confidence limits of BSA on Teflon<sup>®</sup> AF. In contrast, the 10% FBS (multi-component protein solution) on Teflon<sup>®</sup> AF (FBS<sub>10%</sub>) ellipse showed a slightly different localization from the BSA samples (Figure 1B). By examining the first principal component (51% of all the variance in the dataset) exclusively, co-localization of the FBS<sub>10%</sub> with the BSA<sub>Teflon AF</sub> and other BSA samples is noted. Examining the second principal component (17% of the overall variance) exclusively, reveals a higher value for the FBS<sub>10%</sub> compared to the BSA samples. Thus, the analysis requires analysis of the second PC to find differences between the BSA<sub>Teflon</sub> and FBS<sub>10%</sub> surfaces.

To evaluate differences between PCA groupings of proteins, a two-dimensional distance between the centers of each protein grouping shown in Figure 1 was calculated. The average normalized distance of BSA<sub>Teflon AF</sub> to BSA groupings on other substrates was  $0.016 \pm 0.006$ , while the distance between BSA<sub>Teflon AF</sub> to other proteins was  $0.06 \pm 0.03$ . With the exception of transferrin, all other proteins had distances from BSA<sub>Teflon AF</sub> that were greater than 0.04 -- four standard deviations higher than the average BSA distance. Thus, the distance between BSA<sub>Teflon AF</sub> and BSA adsorbed onto other substrates was significantly smaller than that between BSA<sub>Teflon AF</sub> and all other proteins examined except transferrin.

The FBS<sub>10%</sub> distance from the BSA samples was  $0.05 \pm 0.01$ , while the average normalized distance of FBS<sub>10%</sub> to the remaining proteins was  $0.08 \pm 0.04$ . Although this analysis cannot distinguish between proteins *per se* (e.g., transferrin can not be separated from BSA using just the first two PCs), the location of the FBS<sub>10%</sub> relative to BSA and the other proteins indicates that BSA from the FBS solution is a major component of protein film adsorbed onto the Teflon<sup>®</sup> AF surface from this complex solution.

### Fluorescence scanning detection of surface-adsorbed albumin and fibronectin

Results of fluorescence mapping experiments of protein adsorption to various surfaces are shown in Figure 2. Results presented are for equivalent protein concentrations and fluorescence labels by species across all experimental trials (i.e., 4  $\mu\text{g/ml}$  fibronectin-Alexa Fluor 555<sup>®</sup> and 37  $\mu\text{g/ml}$  albumin-Alexa Fluor 647<sup>®</sup>). Significantly, this fibronectin concentration is roughly equivalent to that in 10% FBS (i.e., 10% physiological concentration), whereas the albumin concentration is considerably less than encountered in either circumstance (i.e., 1% of that in 10% FBS, 0.1% of physiological concentration) due to fluorescence signal saturation with albumin at physiological concentration and in 1:10 or 1:100 dilutions.

The highly hydrophilic Codelink<sup>™</sup> hydrogel control surfaces showed minimal protein adsorption (background levels) compared to both glass and highly hydrophobic FC surfaces (Figure 2). As a hydrated, uncharged polyacrylamide-based coating, this commercial microarraying surface is designed to repel serum proteins.<sup>62</sup> Protein adsorption was not significantly different on the Codelink<sup>™</sup> surface based on the protein species (albumin versus fibronectin, Figure 2 insert), very close to background fluorescence (unlabeled protein, Figure 2 insert), reflecting minimal protein adsorption detected on the Codelink<sup>™</sup> surface. Fluorescence intensity assays indicate that albumin inundates FC surfaces, even well below physiological (e.g., at 1/1000<sup>th</sup>) or standard cell culture condition (1/100<sup>th</sup>) levels of protein. Fibronectin is barely detectable on FC samples exposed to binary solutions of fibronectin and albumin (data not shown), consistent with previous reports.<sup>17,19,31,32</sup> Collectively, results of PCA and fluorescence scanning experiments indicate that monocytes/macrophages must *initially* encounter and interact with an albumin-rich FC surface *in vitro* in culture.

### Cell adhesion, growth and proliferation on control and FC substrates

Adhesion, growth and proliferation of (monocyte-) macrophage and fibroblast immortalized cell lines was compared with primary-derived murine BMMO cultures on FC (Teflon<sup>®</sup> AF and pp-FC) using light microscopy techniques. Teflon<sup>®</sup> AF has been employed in previous studies employing monocyte/macrophage,<sup>43,44,63</sup> neuronal<sup>64</sup> and endothelial<sup>65</sup> cells due to its solubility and nearly 100% light transmission, allowing facile microscopic evaluation of cell cultures. Based on our preliminary findings related to cell adhesive behavior,<sup>43,44,63</sup> both FC surface chemistries utilized were predicted to yield similar protein adsorption and cell adhesive patterns, regardless of macrophage cell origin.

Cells were tracked live and after fixation/staining using the Wright-Giemsa technique.<sup>59</sup> As expected, all cells efficiently colonized TCPS control surfaces (Figure 3A, C, E, G, I). On FC surfaces, all (monocyte-) macrophage cells tested also achieved proficient growth and proliferation, although cell adhesion was less than 100% (Figure 3B, D, F and H, spherical cell morphologies are non-adherent). Adherent cells were not easily removed by rinsing and exhibited motile phenotypes, often displaying lengthy filopodia (up to hundreds of microns from the cell body) which appeared to be “probing” the surface in search of adhesive sites.<sup>63</sup> BMMO (Figure 4) and IC-21<sup>63</sup> cell populations on FC surfaces showed a mixture of actin-



based cytoskeletal features (e.g., filopodia, membrane ruffling, Figure 4D and F), often with numerous features on a single cell.

A temporal series of phase contrast photomicrographs for BMMO cell adhesion, growth and proliferation on pp-FC surfaces pre-conditioned with 3 mg/ml BSA, 100% FBS or 10% FBS is shown in Figure 4. By 24 hours, some cells had attached and adopted characteristic adherent macrophage morphologies: astral shapes with short filopodia (Figure 4A–C). At Day 8, adherent macrophages had approximately doubled in size (Figure 4D–F, note scale bar difference) and filopodia and membrane ruffles were observed features of the majority of cells, comparable to previous observations on model biomaterial surfaces.<sup>44,63</sup> Similar surface coverage and growth patterns were observed for each test condition (Figure 4G–I). At Day 12, a substantial portion of each pp-FC surface was covered with cells (Figure 4J, L), although some areas were more sparsely populated (Figure 4K). By Day 19, individual cells adopted macrophage morphologies typically observed on FC surfaces:<sup>44,63</sup> lengthy filopodia, membrane ruffling, unusual shapes and clustered growth with overlapping regions (Figure 4M–O). Generally, BMMO morphologies on pp-FC surfaces were consistent with those previously observed for the IC-21 macrophage cell line on Teflon<sup>®</sup> AF surfaces.<sup>63</sup>

For all time points, cell adhesion results for FC surfaces exposed to 3 mg/ml BSA or 10% FBS were comparable, suggestive of albumin biasing of the protein-adsorbed surface, regardless of whether a complex mixture of serum proteins (e.g., FBS) or a single component BSA solution was used to condition the FC surface prior to cell culture. Results shown in Figure 3 (pp-FC) indicate that this surface supported cell growth and proliferation, but when compared to Teflon<sup>®</sup> AF (Figure 5), a significant difference in BMMO response was observed. Although numerous non-adherent cells were observed on each FC surface (i.e., spherical cells with a haloed appearance), Teflon<sup>®</sup> AF was more permissive to BMMO attachment and spreading; this behavior was observed from 8–36 days of culture. On pp-FC, BMMO grew and proliferated until approximately Day 21 of culture, when cells began to detach and die.

In contrast, attachment-dependent NIH 3T3 fibroblast cells (controls) were unable to colonize identically treated pp-FC surfaces (Figure 3J and Figure 6D–I) at any time point. On PS surfaces (Figure 6A–C) cell proliferative kinetics were approximately equivalent for the 3 mg/ml BSA and 10% FBS samples. PS surfaces pre-conditioned with 100% FBS (Figure 6B) showed substantial improvement in cell proliferation at early time points (through 72 hours). Eventually, the cell populations on all three PS pre-conditioned surfaces reached 100% confluence (data not shown), and large confluent “sheets” of fibroblasts delaminated easily from PS, suggesting that cell-cell contacts were stronger than cell-surface interactions on this surface. On Teflon<sup>®</sup> AF surfaces, BSA and 10% FBS pre-conditioning treatments (Figure 6D and F) also exhibit similar non-adhesive results, with only 100% FBS (Figure 6E) supporting limited NIH 3T3 cell adhesion. The pp-FC surfaces were non-supportive of cell adhesion regardless of pre-conditioning (Figure 6G–I) and this was maintained until NIH 3T3 cultures were terminated (Day 6 post-seeding).

Surface pre-conditioning treatments also included PBS<sup>++</sup>, 0.3 mg/ml fibrinogen (control), 10% HI FBS in PBS<sup>++</sup> and cell-specific medium containing 10% FBS. Regardless of treatment, BMMO (data not shown) and IC-21 cells both adhered rapidly and spread on FC surfaces, exhibiting great variance in cell size (Supplemental Figure 1). Results for BMMO and IC-21 cell response to the most frequently employed pre-conditioning treatments are shown in Figure 7. When compared to TCPS positive controls (Figure 7, A, C) IC-21 cells on Teflon<sup>®</sup> AF surfaces (Figure 7E, G, I) exhibited more motile phenotypic features. In contrast, BMMO cells were larger with more motile phenotypes on TCPS surfaces at this time point (Figure 7, B, D versus F, H, J). In general, less BMMO adhesion was observed on

Teflon<sup>®</sup> AF surfaces than TCPS, whereas IC-21 adhesion was comparable on both surfaces regardless of protein pre-conditioning (Supplemental Figure 2).

### A majority of IC-21 and BMMO cells present Mac 1 integrin subunits

Flow cytometry experiments were performed to determine levels of expression of  $\alpha_2$  and  $\beta_M$  subunits comprising the Mac-1 (CD11b/CD18) integrin receptor in BMMO and IC-21 populations. Results (Figure 8) indicate that  $76 \pm 13\%$  of the IC-21 and  $80 \pm 5\%$  of the BMMO cells express  $\alpha_2$  (CD18), and  $90 \pm 1\%$  of the IC-21 and  $87 \pm 3\%$  of the BMMO populations express  $\beta_M$  (CD11b). Integrin  $\alpha_2$  is often implicated in macrophage adhesion<sup>66</sup> and extravasation.<sup>67</sup> Mac-1 ( $\beta_M/\alpha_2$ ) is known to interact with numerous ligands, including complement protein C3, fibrinogen, ICAM-1, -2 and -3, VCAM-1 and factor X.<sup>68</sup> Further, Mac 1 has been implicated in mediating leukocyte adhesion to denatured proteins, including albumin<sup>69</sup> and denatured albumin,<sup>16</sup> facilitating interactions of cells with solid substrates.<sup>16</sup> Hence, its presence in the majority of these cells implicates a possible mechanism for albumin-based surface adhesion.

### Functional blocking of integrin $\beta_2$ reduces cell adhesion on Teflon<sup>®</sup> AF substrates and leads to altered adherent macrophage morphology

Antibody function-blocking experiments were used to determine the role of  $\alpha_1$  and  $\alpha_2$  integrin subunits on macrophage adhesion to FC surfaces. Controls for 1) the surface, Teflon<sup>®</sup> AF (Figure 9A, D) and 2) non-specific binding (isotype matched control, Rat IgG2a, ; Figure 9B, E) were included. mAb-blocking against integrin  $\alpha_2$  produced significantly reduced cell adhesion for both the IC-21 (reduced  $88 \pm 6\%$ ) and BMMO (reduced  $80 \pm 9\%$ ) cells on Teflon<sup>®</sup> AF surfaces (Figure 9C, F) compared to untreated cells seeded under identical conditions. Further, at one hour post-seeding,  $\alpha_2$ -blocked seeded cells (Figure 9C, F) exhibit altered morphologies when compared to both those unblocked on Teflon<sup>®</sup> AF (Figure 9A, D) and isotype controls (Figure 9B, E). Post-blocking adherent cell morphology was more spherical with fewer obvious adhesion sites, fewer filopodia and less extensive membrane ruffling, reflecting phenotypic change.

Incomplete blocking of cell adhesion observed in this experiment suggests (an) additional mechanism(s) for cell attachment, given that flow cytometry shows 20–24% of the cell populations lack a  $\alpha_2$  receptor, and blocking efficiency directed against  $\alpha_2$  is less than 100%. Other integrins may contribute to monocyte/macrophage adhesion. Analogous assay of  $\alpha_1$  integrin-mediated adhesion were inconclusive due to high levels of non-specific binding for isotype controls (data not shown). Non-integrin mediated cell attachment mechanisms may include non-specific binding, hydrophobic interactions and interactions (primarily electrostatic in nature) between heparin- (or heparin-like) binding domain and proteoglycans or glycoproteins found on cells/surfaces.<sup>68</sup> However, that these are specific to macrophage adhesion on FC, and not other cell types shown refractory to FC binding in serum, seems implausible.

### Fibronectin transcript expression in cells adherent on control and Teflon<sup>®</sup> AF surfaces

Fibronectin mRNA production in both BMMO and IC-21 (Supplemental Figure 3) cells grown on TCPS and Teflon<sup>®</sup> AF surfaces was confirmed at various time points (up to 24-hours post-seeding). Agarose gel electrophoresis results for fibronectin cDNA amplification (Supplemental Figure 3A, lanes 2–5; B lanes 2–4) yielded a 400 bp amplicon band. Each sample was also positive for GAPDH (data not shown). BMMO cells were positive for fibronectin transcript production at 30 and 60 minutes on both surfaces (Supplemental Figure 3A, lanes 2–5); whereas IC-21 cells expressed fibronectin transcript at 30 minutes and two hours post-seeding on TCPS (Supplemental Figure 3B, lanes 2–3) but not Teflon<sup>®</sup> AF (data not shown). IC-21 cells were positive for fibronectin production on Teflon<sup>®</sup> AF,

but only at 24 hours post-seeding (Supplemental Figure 3B, lane 4). Endogenous macrophage fibronectin production demonstrated at early culture time points (30 minutes in some cases, Supplemental Figure 3) may increase adsorbed matrix protein density sufficiently to increase cell adhesive site density, facilitating cell-surface interactions, producing cell-enhanced remodeling of the pre-existing surface adsorbed protein layer and additional monocyte/macrophage adhesion as cultures progress temporally.

## DISCUSSION

Significant to the FBR observed *in vivo* surrounding implanted fluorinated polymers,<sup>3,70</sup> *in vitro* macrophage cultures were found to efficiently adhere to and colonize FC surfaces of two different chemical compositions despite an abundant adsorbed albumin overlayer. This distinct FC adhesive behavior characterized cells of both primary- (BMMO) and secondary- (IC-21) origin. At early time points, BMMO colonization was more successful on standard tissue culture substrates designed to promote cell adhesion, growth and proliferation compared to FC. However, BMMO cells were able to achieve nearly 100% confluent surface coverage on FC substrates as cultures progressed. Both FC substrate cultures were allowed to progress to extended (21–36 day) time points not typically assayed *in vitro*. Some previous reports assay “non-adhesive” albuminated substrates such as FC for very short (~24 hours) time periods,<sup>71</sup> perhaps missing a more long-term efficient cell adhesion to FC surfaces described here. While short-term interactions might be interesting for *in vitro* drug screening assays using macrophages (i.e., for inflammatory mediators), longer-term adhesion in serum is relevant to the FBR scenario. Findings confirm numerous previous reports of “anomalous” monocyte/macrophage growth<sup>41,42</sup> and motility on hydrophobic surfaces<sup>16,33,69</sup> that contrast the better-known poor adhesion characteristics typical of numerous cultured attachment-dependent mammalian cell types on FC surfaces.<sup>15,36,72,73</sup>

Several protein pre-conditioning treatments produced similar effects on observed macrophage adhesion to and colonization of FC substrates, although slightly improved cell adhesion was noted for FC surfaces pre-biased with the known macrophage-adhesive protein<sup>1,74</sup> fibrinogen. Previous studies show unique behavior for proteins in general, and albumin specifically, on FC surfaces.<sup>30–32</sup> As supported by ToF-SIMS data, albumin, the most abundant serum protein (55% of total serum mass),<sup>9</sup> binds to FC surfaces with high affinity and retention, resisting surfactant elution.<sup>23,24,31</sup> This albumin-binding characteristic has been correlated with improved surface resistance to cell adhesion, related to the ability of albumin to effectively block recognition of adhesive protein motifs present on these surfaces via integrin receptor-mediated interactions.<sup>24,31,36,75,76</sup> This is significant given that ToF-SIMS and fluorescence staining show that albumin is the primary adsorbed protein on culture surfaces assessed here and correlated with macrophage adhesion. Other potential adsorbed protein mediators of (monocyte-) macrophage adhesion to FC surfaces *in vitro* include complement protein C3,<sup>66</sup> fibrinogen,<sup>77,78</sup> and trace matrix proteins (e.g., fibronectin and vitronectin),<sup>79,80</sup> each known to interact with cells via specific integrin receptor interactions. However, previous serum-based adsorption studies indicate that negligible serum-adsorbed fibronectin is detectable on PTFE<sup>20</sup> or Teflon<sup>®</sup> AF.<sup>81</sup> Fibrinogen should be effectively removed during standard commercial serum preparation.<sup>82</sup>

Interestingly, despite presumed albumin dominance of FC surfaces in culture media and similarity in general FC surface composition, pp-C<sub>3</sub>F<sub>8</sub> surfaces were less permissive than Teflon<sup>®</sup> AF surfaces to BMMO cultures, suggesting that variations in FC surface chemistry or architecture translate to altered protein conformations that affect these naïve cells in culture. The two FC surfaces likely exhibit different surface and bulk FC chain arrangements: Teflon<sup>®</sup> AF has amorphous –CF<sub>2</sub>– backbone segments dispersed with 2,2-bis (trifluoromethyl)-4,5-difluoro-1,3-dioxane segments that present –CF<sub>3</sub> groups dispersed in

the surface zone (see XPS spectra in Ref. 32). pp-C<sub>3</sub>F<sub>8</sub> FC is an amorphous, crosslinked thin film,<sup>83,84</sup> with different plasma preparation conditions producing differing amounts of -CF<sub>2</sub>- units oriented both in- and out-of- plane at the surface, and varying amounts of co-existing -CF<sub>3</sub> terminal groups.<sup>83</sup> The reported static aqueous contact angle for pp-FC (112°)<sup>81</sup> suggests a terminating surface layer largely of -CF<sub>3</sub> groups. Hence, these pp-FC surfaces have different mixtures of -CF<sub>2</sub>- and -CF<sub>3</sub> chemistry. These FC surface structural differences can translate to non-equivalent adsorbed protein densities<sup>24</sup> and/or conformations.<sup>85,86</sup> Since lower surface energy correlates to higher albumin retention,<sup>24</sup> and FC surfaces are known to both sequester albumin and exhibit poor cell adhesion, different adhesive behaviors observed for BMMO cells (the most naïve and perhaps the most biologically-relevant/stimulus-sensitive cell type explored here) on pp-FC versus Teflon<sup>®</sup> AF surfaces may be attributed to changing albumin adsorbed states on surfaces over time in culture.

Previous findings indicate that monocytes and activated macrophage cell lines adhere proficiently to denatured proteins, including albumin,<sup>16,69</sup> with direct relevance to the scenario described here. Given that: 1) highly hydrophobic surfaces (e.g., FC) have been shown to be albumin selective, 2) albumin is apparently the major protein adsorbed to both FC surfaces, and 3) the mechanism of adhesion to FC surfaces was consistent with findings of Davis,<sup>16</sup> i.e., functional blocking of the Mac-1  $\alpha$ 2 integrin significantly impaired adhesion of BMMO and IC-21 cells to FC substrates, this suggests that these macrophage cells utilize integrin-mediated binding mechanisms primarily to adhere to denatured proteins present on FC surfaces. Importantly, this interaction may proceed via integrin interactions with protein sites exposed only after albumin surface denaturation or altered conformational state(s) are achieved. Nonetheless, presence of surface-adsorbed fibronectin or other ECM protein density sufficient to accommodate integrin attachment cannot be completely ruled out (except in 100% BSA pre-adsorbed cultures), despite the lack of evidence from fluorescence studies and the strong supporting evidence for predominantly albumin-covered surfaces. While mAb blocking experiments directed toward the  $\alpha$ 2 integrin Mac-1 receptor subunit reduced cell adhesion substantially for both primary- and secondary-derived cells on FC substrates, some limited adhesion was still observed, indicating that other interactions mediate macrophage adhesion to FC surfaces. Collectively, these studies demonstrate that primary BMMO and secondary-derived IC-21 cells behave very similarly in their adhesive capacity and mechanism, and cell morphology, motility and proliferative behavior on FC surfaces regardless of protein surface biasing. Differences observed between IC-21 and BMMO cells grown to extended culture times (36 days) on pp-FC and Teflon<sup>®</sup> AF surfaces may reflect important phenotypic differences enhanced by extending culture times. Since many immortalized secondary cells lines are selected for their ability to readily grow in adhesion-dependent cultures, phenotypic differences between primary (i.e., surface naïve) macrophages and those of secondary origin might be attributed to this selection bias.

Lastly, *in vitro* “biocompatibility” testing and cell-based high-throughput drug screening assays (i.e., for inflammatory tests) often employ immortalized, secondary-derived (monocyte-) macrophage cell lines due to their inflammatory phenotype, ready availability, ease of culture, and cost-effectiveness, despite the fact that these cells exhibit varied adhesion patterns, culture requirements, longevity and unknown “equivalence” to primary inflammatory cell phenotypes. Masking agents such as albumin and assay substrate materials including FC are used to prevent undesired cell adhesion to certain assay components in these cultures. This study indicates that this strategy might in fact facilitate unwanted cell adhesion and perhaps undesired activation of these cells, producing assay artifacts not representative of *in vivo* conditions.

## CONCLUSIONS

The major conclusions of this study are that: 1) macrophages readily adhere to and populate albuminated FC surfaces that are non-permissive to other cell types *in vitro*, 2) cells of both primary and secondary (immortalized) origin respond to FC surfaces very similarly over short (<1 week) culture periods, 3) the Mac-1  $\alpha_2$  integrin receptor subunit plays a major role in establishing initial cell adhesive contacts to FC surfaces in the presence of both albumin and serum media, and 4) albumin's use as masking agent in many cell-based assays, drug screening, and as a passivating agent implanted biomaterials might not be advised where macrophage adhesion is undesirable.

## Supplementary Material

Refer to Web version on PubMed Central for supplementary material.

## Acknowledgments

This work was funded by NIH grant EB 000894. ToF-SIMS and PCA experiments were performed at the National ESCA and Surface Analysis Center for Biomedical Problems, funded by NIH grant EB-002027. The authors acknowledge A. García (Georgia Institute of Technology), G. Hagen, P. Gong, P. Wu, M. Gonzalez-Juarero (Colorado State University), M.S. Wagner (Proctor and Gamble) and D.J. Graham (Assemblon, Inc.) for helpful technical guidance. Y-F. "Jerry" Liu is appreciated for technical assistance with RT-PCR experiments.

## References

1. Tang L, Eaton JW. Inflammatory responses to biomaterials. *Am J Clin Pathol.* 1995; 103(4):466–71. [PubMed: 7726145]
2. Anderson JM. Inflammatory response to implants. *ASAIO Trans.* 1988; 34(2):101–7. [PubMed: 3285869]
3. Anderson JM. Biological responses to materials. *Annu Rev Mater Res.* 2001; 31:81–110.
4. Anderson JM. Multinucleated giant cells. *Curr Opin Hematol.* 2000; 7(1):40–7. [PubMed: 10608503]
5. Dadsetan M, Jones JA, Hiltner A, Anderson JM. Surface chemistry mediates adhesive structure, cytoskeletal organization, and fusion of macrophages. *J Biomed Mater Res A.* 2004; 71(3):439–48. [PubMed: 15476262]
6. Horbett TA. The role of adsorbed proteins in animal cell adhesion. *Surf Coll B.* 1994; 2:225–40.
7. Sethuraman A, Han M, Kane RS, Belfort G. Effect of surface wettability on the adhesion of proteins. *Langmuir.* 2004; 20(18):7779–88. [PubMed: 15323531]
8. Anderson NL, Anderson NG. The human plasma proteome: history, character, and diagnostic prospects. *Mol Cell Proteomics.* 2002; 1(11):845–67. [PubMed: 12488461]
9. Andrade JD, Hlady V. Plasma protein adsorption: the big twelve. *Ann N Y Acad Sci.* 1987; 516:158–72. [PubMed: 3439723]
10. Haynes CA, Norde W. Globular proteins at solid/liquid interfaces. *Coll Surf B.* 1994; 2:517–66.
11. Horbett TA. Principles underlying the role of adsorbed plasma proteins in blood interactions with foreign materials. *Cardiovasc Pathol.* 1993; 2:137S–148S.
12. Norde W. Adsorption of proteins from solution at the solid-liquid interface. *Adv Colloid Interface Sci.* 1986; 25(4):267–340. [PubMed: 3333131]
13. Garcia AJ, Vega MD, Boettiger D. Modulation of cell proliferation and differentiation through substrate-dependent changes in fibronectin conformation. *Mol Biol Cell.* 1999; 10(3):785–98. [PubMed: 10069818]
14. Iuliano DJ, Saavedra SS, Truskey GA. Effect of the conformation and orientation of adsorbed fibronectin on endothelial cell spreading and the strength of adhesion. *J Biomed Mater Res.* 1993; 27(8):1103–13. [PubMed: 8408123]



15. Dewez JL, Doren A, Schneider YJ, Rouxhet PG. Competitive adsorption of proteins: key of the relationship between substratum surface properties and adhesion of epithelial cells. *Biomaterials*. 1999; 20(6):547–59. [PubMed: 10213358]
16. Davis GE. The Mac-1 and p150,95 beta 2 integrins bind denatured proteins to mediate leukocyte cell-substrate adhesion. *Exp Cell Res*. 1992; 200(2):242–52. [PubMed: 1572393]
17. Baszkin A, Lyman DJ. The interaction of plasma proteins with polymers. I. Relationship between polymer surface energy and protein adsorption/desorption. *J Biomed Mater Res*. 1980; 14(4):393–403. [PubMed: 6156944]
18. Keogh J, Eaton J. Albumin affinity for biomaterial surfaces. *Cells and Materials*. 1996; 6(1–3): 209–220.
19. Lassen B, Malmsten M. Competitive protein adsorption at radio frequency plasma polymer surfaces. *J Mater Sci Mater Med*. 1994; 5:662–665.
20. Wagner MS, Horbett TA, Castner DG. Characterization of the structure of binary and ternary adsorbed protein films using electron spectroscopy for chemical analysis, time-of-flight-secondary ion mass spectrometry, and radiolabeling. *Langmuir*. 2003; 19:1708–15.
21. Wagner MS, Castner DG. Characterization of adsorbed protein films by time-of-flight secondary ion mass spectrometry with principal component analysis. *Langmuir*. 2001; 17(15):4649–4660.
22. McFarland CD, De Filippis C, Jenkins M, Tunstall A, Rhodes NP, Williams DF, Steele JG. Albumin-binding surfaces: in vitro activity. *J Biomater Sci Polym Ed*. 1998; 9(11):1227–39. [PubMed: 9860182]
23. Bohnert JL, Fowler BC, Horbett TA, Hoffman AS. Plasma gas discharge deposited fluorocarbon polymers exhibit reduced elutability of adsorbed albumin and fibrinogen. *J Biomater Sci Polym Ed*. 1990; 1(4):279–97. [PubMed: 2149071]
24. Kiaei D, Hoffman AS, Horbett TA. Tight binding of albumin to glow discharge treated polymers. *J Biomater Sci Polym Ed*. 1992; 4(1):35–44. [PubMed: 1463700]
25. Eberhart RC, Prokop LD, Wissenger J, Wilkov MA. Observation of albumin deposits on teflon surfaces. *Trans Am Soc Artif Intern Organs*. 1977; 23:134–40. [PubMed: 910327]
26. Eberhart RC. Albumin adsorption and retention on C18-alkyl-derivatized polyurethane vascular grafts. *Artif Organs*. 1987; 11(5):375–82. [PubMed: 3689173]
27. Absolom DR, Zingg W, Neumann AW. Protein adsorption to polymer particles: role of surface properties. *J Biomed Mater Res*. 1987; 21(2):161–71. [PubMed: 3818679]
28. Kim SW, Lee RG, Oster H, Coleman D, Andrade JD, Lentz DJ, Olsen D. Platelet adhesion to polymer surfaces. *Trans Am Soc Artif Intern Organs*. 1974; 20(B):449–55. [PubMed: 4141527]
29. Zucker MB, Vroman L. Platelet adhesion induced by fibrinogen adsorbed onto glass. *Proc Soc Exp Biol Med*. 1969; 131(2):318–20. [PubMed: 5305877]
30. Lateef S, Boateng S, Ahluwalia N, Hartman T, Russell B, Hanley L. Three-dimensional chemical structures by protein functionalized micron-sized beads bound to polylysine-coated silicone surfaces. *J Biomed Mater Res*. 2005; 72A:373–380.
31. Grainger DW, Pavon-Djavid G, Migonney V, Josefowicz M. Assessment of fibronectin conformation adsorbed to polytetrafluoroethylene surfaces from serum protein mixtures and correlation to support of cell attachment in culture. *J Biomater Sci Polym Ed*. 2003; 14(9):973–88. [PubMed: 14661874]
32. Koenig AL, Gambillara V, Grainger DW. Correlating fibronectin adsorption with endothelial cell adhesion and signaling on polymer substrates. *J Biomed Mater Res A*. 2003; 64(1):20–37. [PubMed: 12483693]
33. Rich A, Harris AK. Anomalous preferences of cultured macrophages for hydrophobic and roughened substrata. *J Cell Sci*. 1981; 50:1–7. [PubMed: 7033247]
34. Schakenraad JM, Busscher HJ, Wildevuur CR, Arends J. The influence of substratum surface free energy on growth and spreading of human fibroblasts in the presence and absence of serum proteins. *J Biomed Mater Res*. 1986; 20(6):773–84. [PubMed: 3722214]
35. van Kooten, TG. *Encyclopedia of Surface and Colloid Science*. New York, NY: Marcel Dekker, Inc; 2004. Growth of cells on polymer surfaces; p. 1-19.

36. Webb K, Hlady V, Tresco PA. Relative importance of surface wettability and charged functional groups on NIH 3T3 fibroblast attachment, spreading, and cytoskeletal organization. *J Biomed Mater Res.* 1998; 41(3):422–30. [PubMed: 9659612]
37. Weisiger R, Gollan J, Ockner R. Receptor for albumin on the liver cell surface may mediate uptake of fatty acids and other albumin-bound substances. *Science.* 1981; 211(4486):1048–51. [PubMed: 6258226]
38. Tiruppathi C, Finnegan A, Malik AB. Isolation and characterization of a cell surface albumin-binding protein from vascular endothelial cells. *Proc Natl Acad Sci U S A.* 1996; 93(1):250–4. [PubMed: 8552615]
39. Chaudhury C, Mehnaz S, Robinson JM, Hayton WL, Pearl DK, Roopenian DC, Anderson CL. The major histocompatibility complex-related Fc receptor for IgG (FcRn) binds albumin and prolongs its lifespan. *J Exp Med.* 2003; 197(3):315–22. [PubMed: 12566415]
40. Zhu X, Meng G, Dickinson BL, Li X, Mizoguchi E, Miao L, Wang Y, Robert C, Wu B, Smith PD, et al. MHC class I-related neonatal Fc receptor for IgG is functionally expressed in monocytes, intestinal macrophages, and dendritic cells. *J Immunol.* 2001; 166(5):3266–76. [PubMed: 11207281]
41. Andreesen R, Gadd S, Brugger W, Lohr GW, Atkins RC. Activation of human monocyte-derived macrophages cultured on Teflon: response to interferon-gamma during terminal maturation in vitro. *Immunobiology.* 1988; 177(2):186–98. [PubMed: 3136081]
42. Andreesen R, Picht J, Lohr GW. Primary cultures of human blood-born macrophages grown on hydrophobic teflon membranes. *J Immunol Methods.* 1983; 56(3):295–304. [PubMed: 6833764]
43. Godek ML, Duchsherer NL, McElwee Q, Grainger DW. Morphology and growth of murine cell lines on model biomaterials. *Biomed Sci Instrum.* 2004; 40:7–12. [PubMed: 15133927]
44. Godek ML, Malkov GM, Fisher ER, Grainger DW. Macrophage serum-based adhesion to plasma-processed surface chemistry is distinct from that exhibited by fibroblasts. *Plasma Proc Polym.* 2006; 3:485–497.
45. Mael J, Defendi V. Infection and transformation of mouse peritoneal macrophages by simian virus 40. *J Exp Med.* 1971; 134(2):335–50. [PubMed: 4326994]
46. Springer TA. Traffic signals for lymphocyte recirculation and leukocyte emigration: the multistep paradigm. *Cell.* 1994; 76(2):301–14. [PubMed: 7507411]
47. Alitalo K, Hovi T, Vaheri A. Fibronectin is produced by human macrophages. *J Exp Med.* 1980; 151(3):602–13. [PubMed: 7359083]
48. Hershkovitz R, Alon R, Gilat D, Lider O. Activated T lymphocytes and macrophages secrete fibronectin which strongly supports cell adhesion. *Cell Immunol.* 1992; 141(2):352–61. [PubMed: 1576655]
49. Nathan CF. Secretory Products of Macrophages. *J Clin Invest.* 1987; 79:319–326. [PubMed: 3543052]
50. Lewis C, McCarthy S, Lorenzen J, McGee Jd. Differential effects of LPS, IFN-gamma and TNFalpha on the secretion of lysozyme by individual human mononuclear phagocytes: relationship to cell maturity. *Immunology.* 1990; 69(3):402–408. [PubMed: 2107146]
51. Malkov G, Martin IT, Schwisow WB, Chandler JP, Fisher ER. Pulsed plasma-induced micropatterning with alternating hydrophilic and hydrophobic surface chemistries. *Chem Mater.* 2005 submitted.
52. Canavan HE, Graham DJ, Cheng X, Ratner BD, Castner DG. Comparison of Native Extracellular Matrix with Adsorbed Protein Films using Secondary Ion Mass Spectrometry. *Langmuir.* 2007; 23:50–56. [PubMed: 17190484]
53. Sanni OD, Wagner MS, Briggs D, Castner DG, Vickerman JC. Classification of adsorbed protein static ToF-SIMS spectra by principal component analysis and neural networks. *Surf Interf Anal.* 2002; 33:715–728.
54. Lhoest JB, Wagner MS, Tidwell CD, Castner DG. Characterization of adsorbed protein films by time of flight secondary ion mass spectrometry. *Journal of Biomedical Materials Research.* 2001; 57(3):432–440. [PubMed: 11523038]
55. Jackson, J. *A User's Guide to Principal Components.* New York: John Wiley & Sons; 1991.

56. Wagner M, Tyler B, Castner D. Interpretation of ToF-SIMS spectra of adsorbed protein films by multivariate pattern recognition. *Anal Chem.* 2002; 74:1824–1835. [PubMed: 11985314]
57. Kaltenbach JP, Kaltenbach MH, Lyons WB. Nigrosin as a dye for differentiating live and dead ascites cells. *Exp Cell Res.* 1958; 15(1):112–7. [PubMed: 13574164]
58. Rhoades ER, Orme IM. Similar responses by macrophages from young and old mice infected with *Mycobacterium tuberculosis*. *Mech Ageing Dev.* 1998; 106(1–2):145–53. [PubMed: 9883979]
59. Woronzoff-Dashkoff KK. The wright-giemsas stain. *Secrets revealed Clin Lab Med.* 2002; 22(1): 15–23.
60. Bohnsack BL, Lai L, Dolle P, Hirschi KK. Signaling hierarchy downstream of retinoic acid that independently regulates vascular remodeling and endothelial cell proliferation. *Genes Dev.* 2004; 18(11):1345–58. [PubMed: 15175265]
61. Graham D, Wagner M, Castner D. Information from complexity: Challenges of ToF-SIMS data interpretation. *Appl Surf Sci.* 2006; 252:6860–6868.
62. Gong P, Harbers GM, Grainger DW. Multi-technique comparison of immobilized and hybridized oligonucleotide surface density on commercial amine-reactive microarray slides. *Anal Chem.* 2006; 78(7):2342–51. [PubMed: 16579618]
63. Godek ML, Sampson JA, Duchsherer ML, McElwee Q, Grainger DW. Rho GTPase protein expression and activation in murine monocyte/macrophages is not modulated by model biomaterial culture surfaces *in vitro*. *J Biomater Sci Polym Ed.* 2006; 17(10):1141–1158. [PubMed: 17235380]
64. Makohliso SA, Giovangrandi L, Leonard D, Mathieu HJ, Ilegems M, Aebischer P. Application of Teflon-AF thin films for bio-patterning of neural cell adhesion. *Biosens Bioelectron.* 1998; 13(11): 1227–35. [PubMed: 9871978]
65. Anamelechi CC, Truskey GA, Reichert WM. Mylar and Teflon-AF as cell culture substrates for studying endothelial cell adhesion. *Biomaterials.* 2005; 26(34):6887–96. [PubMed: 15990164]
66. McNally AK, Anderson JM. Beta1 and beta2 integrins mediate adhesion during macrophage fusion and multinucleated foreign body giant cell formation. *Am J Pathol.* 2002; 160(2):621–30. [PubMed: 11839583]
67. Luscinskas FW, Kansas GS, Ding H, Pizcueta P, Schleiffenbaum BE, Tedder TF, Gimbrone MA Jr. Monocyte rolling, arrest and spreading on IL-4-activated vascular endothelium under flow is mediated via sequential action of L-selectin, beta 1-integrins, and beta 2-integrins. *J Cell Biol.* 1994; 125(6):1417–27. [PubMed: 7515891]
68. Harbers, GM.; Grainger, DW. Cell-Material Interactions: Fundamental Design Issues for Tissue Engineering and Clinical Considerations. In: Guelcher, SA.; Hollinger, JO., editors. *An Introduction to Biomaterials*. Boca Raton: CRC Press; 2006. p. 15-45.
69. Koyama Y, Norose-Toyoda K, Hirano S, Kobayashi M, Ebihara T, Someki I, Fujisaki H, Irie S. Type I collagen is a non-adhesive extracellular matrix for macrophages. *Arch Histol Cytol.* 2000; 63(1):71–9. [PubMed: 10770590]
70. Williams, DF.; Homsy, CA. *Biocompatibility of Clinical Implant Materials*. Boca Raton, FL: CRC Press; 1981. p. 60-77.
71. Shen M, Horbett TA. The effects of surface chemistry and adsorbed proteins on monocyte/macrophage adhesion to chemically modified polystyrene surfaces. *J Biomed Mater Res.* 2001; 57(3):336–45. [PubMed: 11523028]
72. Ruardy TG, Schakenraad JM, van der Mei HC, Busscher HJ. Adhesion and spreading of human skin fibroblasts on physicochemically characterized gradient surfaces. *J Biomed Mater Res.* 1995; 29(11):1415–23. [PubMed: 8582910]
73. McClary KB, Ugarova T, Grainger DW. Modulating fibroblast adhesion, spreading, and proliferation using self-assembled monolayer films of alkythiolates on gold. *J Biomed Mater Res.* 2000; 50(3):428–39. [PubMed: 10737886]
74. Altieri DC, Agbanyo FR, Plescia J, Ginsberg MH, Edgington TS, Plow EF. A unique recognition site mediates the interaction of fibrinogen with the leukocyte integrin Mac-1 (CD11b/CD18). *J Biol Chem.* 1990; 265(21):12119–22. [PubMed: 1973686]
75. Pitt WG, Cooper SL. Albumin adsorption on alkyl chain derivatized polyurethanes: I. The effect of C-18 alkylation. *J Biomed Mater Res.* 1988; 22(5):359–82. [PubMed: 3397377]

76. Pitt WG, Grasel TG, Cooper SL. Albumin adsorption on alkyl chain derivatized polyurethanes. II. The effect of alkyl chain length. *Biomaterials*. 1988; 9(1):36–46. [PubMed: 3349120]
77. Tang L, Eaton JW. Natural responses to unnatural materials: A molecular mechanism for foreign body reactions. *Mol Med*. 1999; 5(6):351–8. [PubMed: 10415159]
78. Flick MJ, Du X, Witte DP, Jirouskova M, Soloviev DA, Busuttill SJ, Plow EF, Degen JL. Leukocyte engagement of fibrin(ogen) via the integrin receptor  $\alpha$ 5 $\beta$ 1 is critical for host inflammatory response in vivo. *J Clin Invest*. 2004; 113(11):1596–606. [PubMed: 15173886]
79. Underwood PA, Bennett FA. A comparison of the biological activities of the cell-adhesive proteins vitronectin and fibronectin. *J Cell Sci*. 1989; 93(Pt 4):641–9. [PubMed: 2481683]
80. Hayman EG, Pierschbacher MD, Suzuki S, Ruoslahti E. Vitronectin--a major cell attachment-promoting protein in fetal bovine serum. *Exp Cell Res*. 1985; 160(2):245–58. [PubMed: 2412864]
81. Malkov G, Martin IT, Schwisow WB, Chandler JP, Fisher ER. Pulsed plasma-induced micropatterning with alternating hydrophilic and hydrophobic surface chemistries. *Plasma Proc Polym*. 2008 In press.
82. Horbett, TA. Personal communication. 2006.
83. Martin IT, Malkov G, Butoi CI, Fisher ER. Comparison of pulsed and downstream deposition of fluorocarbon materials from  $C_3F_8$  and  $c-C_4F_8$  plasmas. *J Vac Sci Technol*. 2004; 22(2):227–235.
84. Haidopoulos M, Turgeon S, Laroche G, Mantovani D. Chemical and morphological characterization of ultra-thin fluorocarbon plasma-polymer deposition on 316 stainless steel substrates: a first step toward the improvement of the long-term safety of coated stents. *Plasma Proc Polym*. 2004; 2:424–440.
85. Lewis D, Whateley TL. Adsorption of enzymes at the solid-liquid interface. I. Trypsin on polystyrene latex. *Biomaterials*. 1988; 9(1):71–5. [PubMed: 3349124]
86. Sandwick R, Schray K. Conformational states of enzymes bound to surfaces. *J Coll Interface Sci*. 1988; 121:1–12.

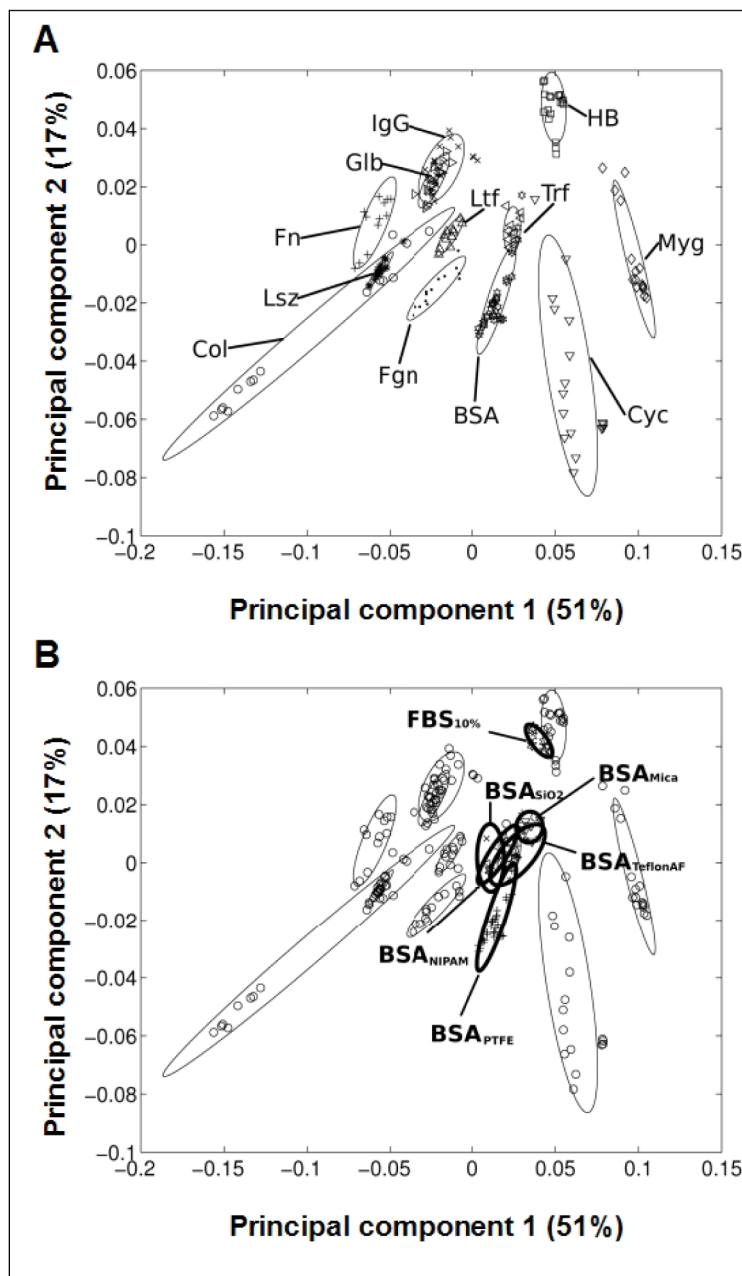


**Figure 1.** ToF-SIMS principal component analysis (PCA) performed on BSA- and 10% FBS-treated Teflon® AF surfaces, projected into the model of Wagner *et al.*<sup>21</sup> A) Wagner's PCA-based model identifying and grouping various proteins adsorbed to PTFE. Abbreviations: collagen (Col), cytochrome C (Cyc), fibrinogen (Fgn), fibronectin (Fn), (gamma)-globulin (Glb), hemoglobin (HB), immunoglobulin G (IgG), lysozyme (Lsz), lactoferrin (Ltf), myoglobin (Myg), transferrin (Trf). B) Samples of 3 mg/ml BSA and 10% FBS adsorbed on Teflon® AF substrates were analyzed by ToF-SIMS and projected into Wagner's BSA model for other substrates.



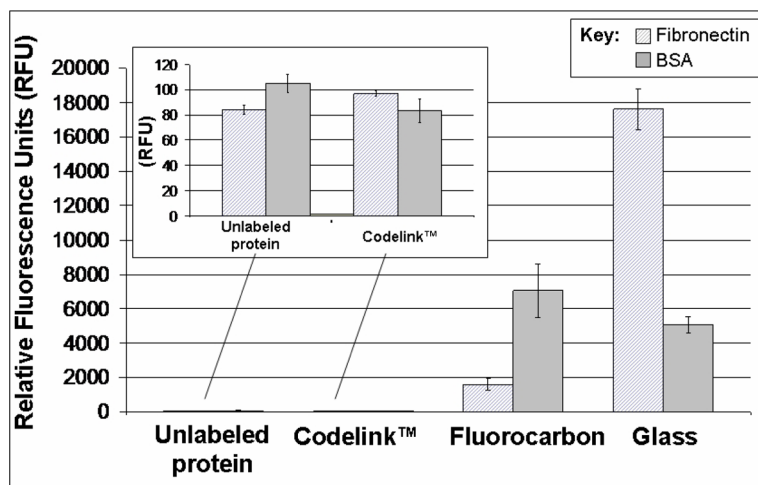


**Figure 2.** Fluorescence scanning results for Alexa Fluor®-labeled (as described in Material and Methods) fibronectin and BSA protein solutions (37  $\mu\text{g/ml}$  BSA-Alexa Fluor 647®, and 4  $\mu\text{g/ml}$  fibronectin-Alexa Fluor 555®) exposed to surfaces with a wide range of wettabilities for 24 hours: Codelink™ and glass controls (very hydrophilic), FC (very hydrophobic). Unlabeled proteins were incubated with FC surfaces as a negative control. Inset: Magnified results for unlabeled protein samples and labeled proteins exposed to hydrophilic Codelink™ substrates.

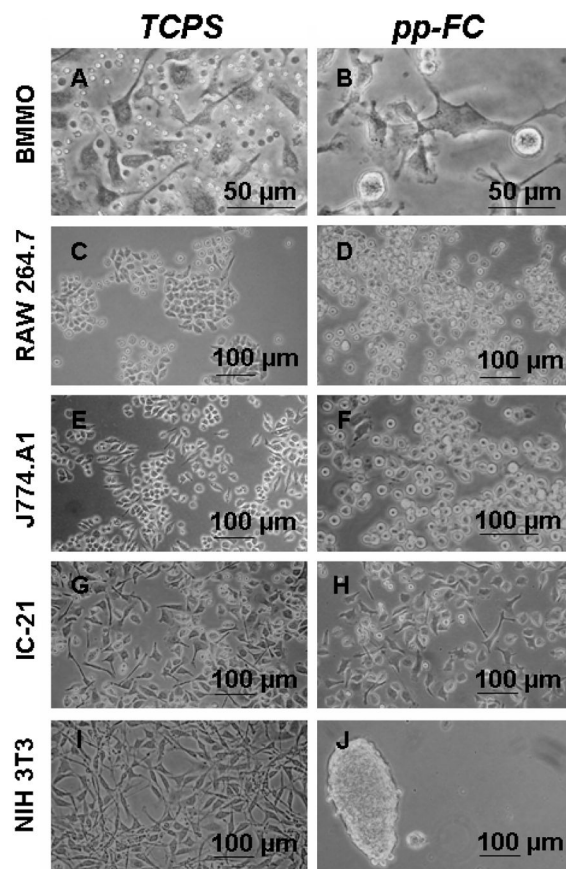


**Figure 3.** Phase contrast photomicrographs of live cells on control (TCPS) and pp-FC surfaces for primary-derived cells (BMMO) and secondary-derived immortalized cell lines of (monocyte-) macrophage (RAW 264.7, J774A.1, IC-21) and fibroblast (NIH 3T3) origin. Cell seeding density varied, as described in Materials and Methods. Cultures depicted represent 2–4 days post-seeding on each surface and represent the typical sub-confluent growth pattern observed for each cell type (except J). Images are representative of multiple fields ( 3) and multiple replicates ( 2) for each test condition.

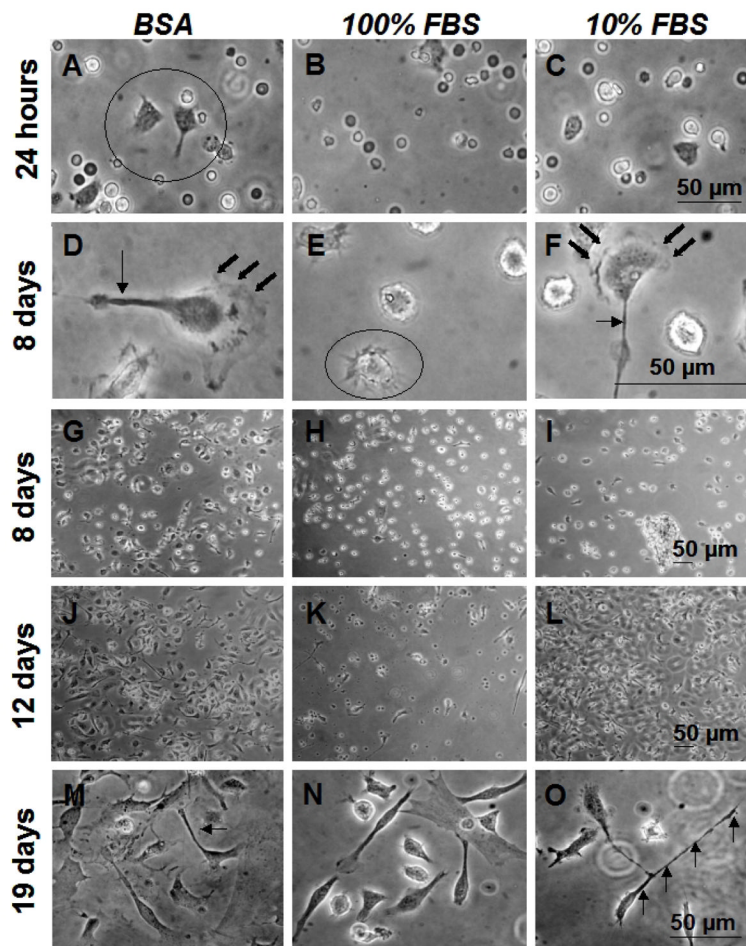


**Figure 4.**

Phase contrast photomicrographs of live BMMO grown on uniform pp-FC surfaces preconditioned with a single component BSA (3 mg/ml) solution, 100% FBS or 10% FBS. Cells were seeded at densities of 1500 cells/mm<sup>2</sup> Times indicated and scale bars are relevant for each row of images. Circles indicate “astral” morphology (A, E), arrows indicate filopodia (D, F, M, O) and bold arrows indicate membrane ruffling (D, F). Multiple cytoskeletal features (i.e., filopodia, membrane ruffling) are common features on many cells (e.g., D and F). Images are representative of multiple fields ( 3) and multiple replicates ( 2) for each test condition.

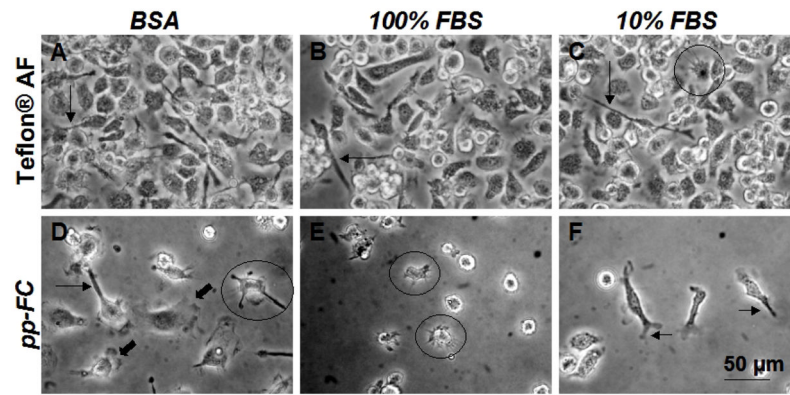


**Figure 5.** Phase contrast photomicrographs of live BMMO (Day 8 in culture) on FC surfaces exposed to preconditioning treatments as indicated. Cells were seeded at densities of 600 cells/mm<sup>2</sup> on Teflon® AF and 1500 cells/mm<sup>2</sup> on pp-FC. Circles indicate astral morphology (C–E), arrows indicate filopodia (A–D, F) and bold arrows indicate membrane ruffling (D). Scale bar shown in F is relevant for all images. Images are representative of multiple fields ( 3) and multiple replicates ( 2) for each test condition.

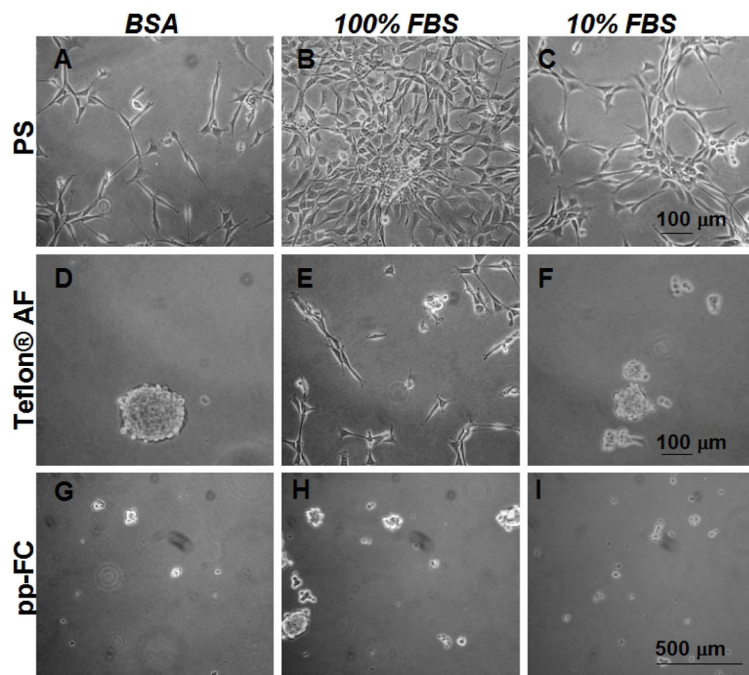


**Figure 6.** Phase contrast photomicrographs of live NIH 3T3 cells 48 hours post-seeding in 10% serum containing media on uniform pp-FC surfaces pre-treated with (3 mg/ml) BSA (A, D and G), 100% (B, E and H) or 10% serum (C, F and I). NIH 3T3 fibroblasts fail to effectively colonize FC surfaces under any of the conditions tested (D–I). Scale bars are relevant for each row. Images are representative of multiple fields (> 5) and multiple plates (2) for each test condition.



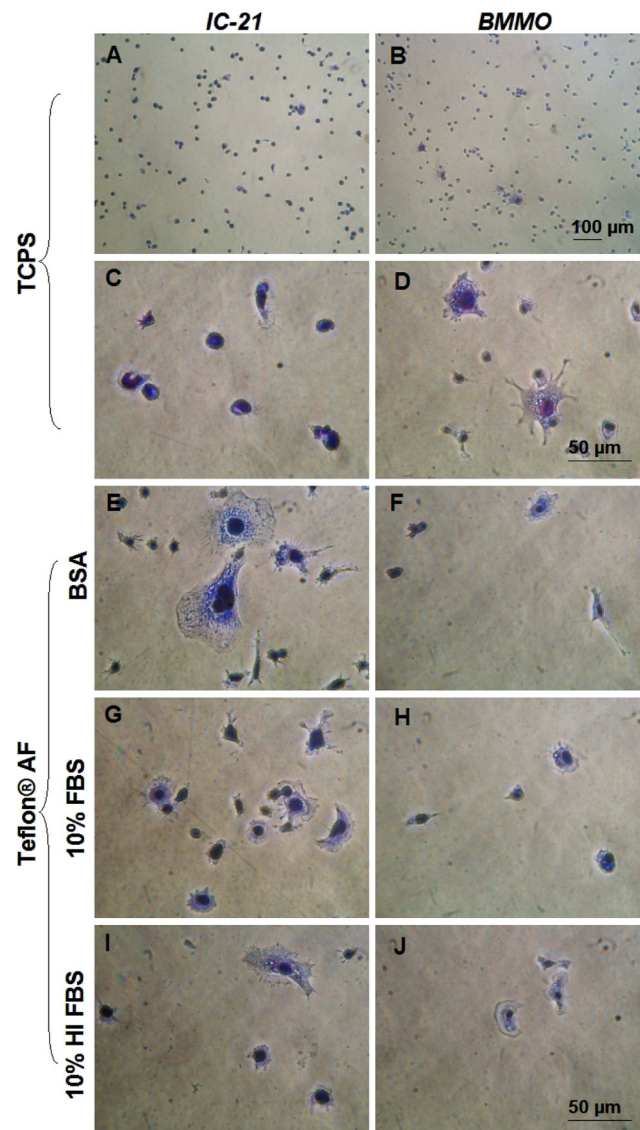


**Figure 7.** Phase contrast photomicrographs of IC-21 and BMMO cells on control (TCPS) and Teflon® AF surfaces with preconditioning treatments (Teflon® AF only) as indicated. Cells were seeded at a density of 500 cells/mm<sup>2</sup>, fixed and stained after one hour. Scale bars in D and J are equivalent, and relative for all panels except A and B. Images are representative of multiple fields ( 3) and multiple replicates ( 2) for each test condition.

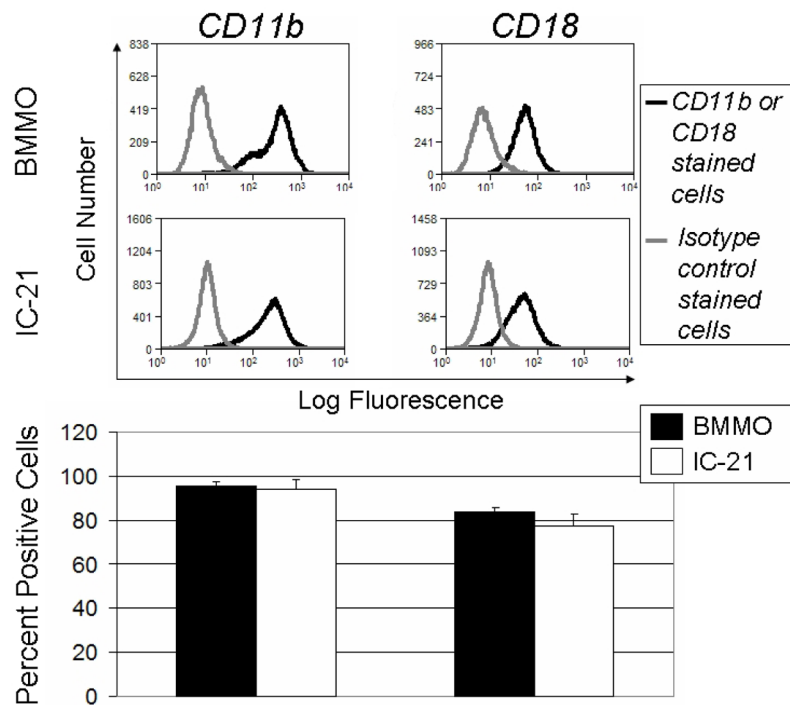


**Figure 8.** Flow cytometry analysis of integrin  $\alpha_2$  (CD18) and  $\alpha_M$  (CD11b) expression on populations of BMMO and IC-21 cells grown on TCPS under standard conditions. A) Histograms showing specific integrin labeling. Black line represents isotype control and dotted line represents fluorescence intensity expressed by binding of isotype control or integrin of interest (CD18, CD 11b) to BMMO or IC-21 cells, respectively. B) Bar graphs representation of data shown in A, indicating the percent of total sampled cell population positive for the integrin indicated.  $n=3$  for each experiment, error bars represent standard error of the mean.

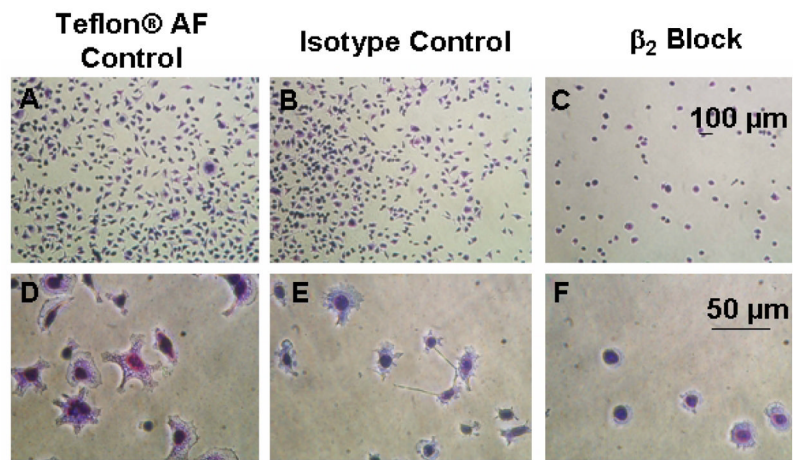


**Figure 9.**

Phase contrast photomicrographs of results for control and  $\beta_2$  blocks performed on IC-21 cells grown on Teflon® AF surfaces preconditioned with 10% FBS. Cells were incubated without antibodies or with either isotype control or blocking antibodies at a concentration of 100  $\mu\text{g}/\text{ml}$  for 30 minutes prior to seeding at a density of 500 cells/ $\text{mm}^2$ . Cells were fixed and stained after one hour. Scale bars are relevant for each row. Images are representative of multiple fields ( 3) and multiple replicates ( 2) for each test condition.